

Article

Synthesis of Diblock Copolymer Consisting of Poly(4-butyltriphenylamine) and Morphological Control in Photovoltaic Application

Kousuke Tsuchiya *, Tatsuro Kikuchi, Malee Songeun, Takeshi Shimomura and Kenji Ogino *

Graduate School of Bio-Applications and Systems Engineering, Tokyo University of Agriculture and Technology, 2-24-16 Nakacho, Koganei-shi, Tokyo 184-8588, Japan;

E-Mails: 50005253014@st.tuat.ac.jp (T.K.); 50008253505@st.tuat.ac.jp (M.S.);

simo@cc.tuat.ac.jp (T.S.)

* Authors to whom correspondence should be addressed; E-Mails: ktsuchiy@cc.tuat.ac.jp (K.T.); kogino@cc.tuat.ac.jp (K.O.); Tel.: +81-42-388-7404; Fax: +81-42-388-7404.

Received: 23 May 2011; in revised form: 8 June 2011 / Accepted: 28 June 2011 /

Published: 1 July 2011

Abstract: The diblock copolymer PTPA-*b*-PS consisting of poly(4-butyltriphenylamine) (PTPA) and polystyrene was prepared by atom transfer radical polymerization followed by C–N coupling polymerization. Three types of block copolymers with different contents of polystyrene segment were prepared. The formation of block copolymer was confirmed by ¹H NMR spectra and gel permeation chromatography (GPC) profiles. Time of flight (TOF) measurement revealed that the block copolymer showed higher hole mobility up to 1.3×10^{-4} cm²/Vs compared with PTPA homopolymer. The surface morphology of block copolymer films blended with [6,6]-phenyl-C₆₁-butyric acid methyl ester (PCBM) was investigated by Atomic force microscopy (AFM). Introduction of polystyrene segment provided microphase-separated structures with domain sizes of around 20 nm. The photovoltaic device based on PTPA-*b*-PS, PTPA, and PCBM exhibited higher efficiency than that of homopolymer blend system.

Keywords: poly(triphenylamine); block copolymer; morphology; hole mobility; photovoltaic cell

1. Introduction

Polymer solar cells are promising as an alternative clean energy source for limited fossil fuels. A mixture of donor and acceptor materials is generally used for the thin photocurrent generating layer of polymer photovoltaic devices. The organic semiconducting polymers, especially for p-type polymers, have been intensively developed as photoactive materials [1,2]. For instance, photovoltaic devices based on regioregular poly(3-hexylthiophene) (P3HT) blended with a fullerene derivative, [6,6]-phenyl-C₆₁-butyric acid methyl ester (PCBM), have been widely studied to give power conversion efficiency, successfully reaching almost 5% [3-7]. The high conversion efficiency achieved by such a blending system was assumably attributed to a phase-separated structure of donor and acceptor materials within tens of nanometer scale, generally called bulk heterojunction. The domain size in the bulk heterojunction matches the diffusion length of drifting excitons generated by light absorption [8]. Therefore, the precise control of the morphology in the polymer layer is essential for improving the conversion efficiency of the device. Recent works on polymer solar cells have addressed this issue by means of additional processes such as thermal [9-12] or solvent vapor annealing [13]. These methods significantly improve the conversion efficiency, with process conditions strictly optimized.

Block copolymers are quite attractive materials for polymer photovoltaic devices because they exhibit a variety of microphase-separated structures such as sphere, cylinder, and lamella. Microphase separation, which possesses a domain size of less than tens of nanometer and a large interfacial area, can offer suitable structures for exciton diffusion as well as charge separation in photovoltaic device. In addition, the morphology is thermodynamically stable enough to improve device durability compared with that in polymer blends. In order to utilize the polymer layer in organic solar cells, numerous block copolymers comprised of p-type segments such as polythiophene and poly(phenylene vinylene) have been prepared [14-29]. Some researchers reported the block copolymers consisting of p- and n-type segments in which fullerene [16,17,27] or perylenediimide [18,24-26] moiety was introduced into the n-type block. Another approach utilized the block copolymers based on crystalline and amorphous p-type segments [19,23,28]. Chueh *et al.* demonstrated that higher efficiency was achieved by the P3HT/PCBM device using poly(4-vinyltriphenylamine)-*b*-poly(3-hexylthiophene)-*b*-poly(4-vinyltriphenylamine) as a surfactant for controlling the inner structure [28].

The functional polymers based on aromatic amines such as triphenylamine or carbazole have been widely developed for electronic devices [30-37]. The block copolymers containing triphenylamine and perylenediimide as side groups were also prepared [14,15]. Poly(triphenylamine)s (PTPAs) were firstly prepared by oxidative coupling polymerization of triphenylamine derivatives, and it was found that soluble poly(4-butyltriphenylamine) showed high hole mobility and high photoconductivity [38,39]. Recently, we have developed novel synthetic route for the preparation of PTPA utilizing palladium-catalyzed C–N coupling polymerization [40]. By adding a terminal modifier consisting of poly(ethylene oxide) (PEO), the diblock copolymer poly(4-butyltriphenylamine)-*b*-poly(ethylene oxide) (PTPA-*b*-PEO) was easily synthesized.

Previously we demonstrated that the hole transporting diblock copolymer P3HT-*b*-PEO was synthesized by coupling regioregular P3HT and PEO homopolymers, and that the morphology can be controlled in the thin films of P3HT-*b*-PEO blended with PCBM [41]. We here report that a novel

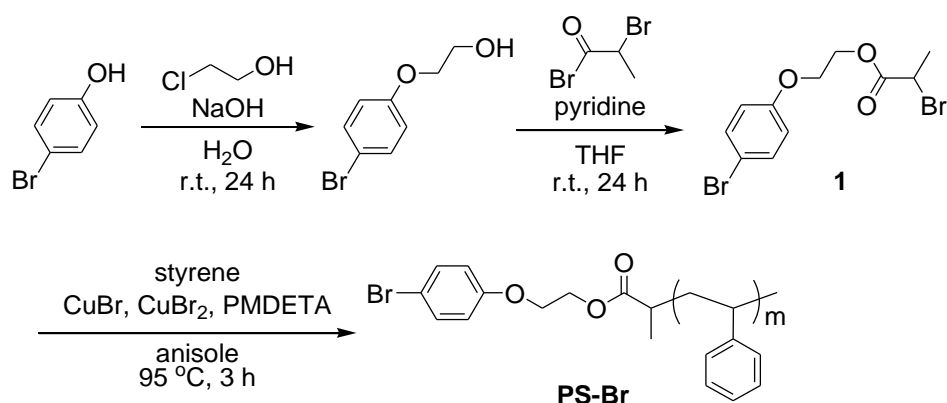
block copolymer consisting of PTPA and polystyrene (PS) was prepared for the application to photovoltaic device. The formation of block copolymer with PS soft segment, which shows high miscibility with PCBM, will assist in controlling the morphology in the device by a microphase separation. The morphologies constructed in the block copolymer blend films were investigated by Atomic force microscopy (AFM) measurement. Furthermore, a correlation between the morphologies and the device performances were discussed for the devices based on block copolymer blends.

2. Results and Discussion

2.1. Synthesis of Diblock Copolymer PTPA-*b*-PS

In our study to utilize microphase-separated structure for photovoltaic device, a diblock copolymer based on poly(butyltriphenylamine) as a hole transporting segment was designed and synthesized by means of palladium C–N coupling polymerization. Previously, using a poly(ethylene oxide) terminal modifier, we have successfully prepared the diblock copolymer poly(butyltriphenylamine)-*b*-poly(ethylene oxide) (PTPA-*b*-PEO) [40]. In this article, 2-bromopropionate derivative (**1**) as an initiator for atom transfer radical polymerization (ATRP) with bromophenyl moiety was synthesized in two step reactions in order to introduce vinylpolymer at one terminal of PTPA (Scheme 1). Taking its good compatibility with PCBM into account, PS was selected as the other segment. The PS terminal modifier (**PS-Br**) was synthesized by ATRP initiated from **1** using CuBr/CuBr₂/PEDMTA catalytic system as reported elsewhere [42]. Two kinds of **PS-Br** with different number average molecular weights ($M_n = 2,300$ and $4,300$) were prepared.

Scheme 1. Syntheses of atom transfer radical polymerization (ATRP) initiator (**1**) and polystyrene (PS) with 4-bromophenyl group at a terminal (**PS-Br**).



C–N coupling polymerization of self-condensing monomer **2** was carried out in the presence of **PS-Br** as a terminal modifier to afford the diblock copolymers consisting of PTPA and PS segments (Scheme 2). Using different **PS-Br** or changing the amount of **PS-Br**, three kinds of **PTPA-*b*-PS** with different weight ratios of PS were prepared as shown in Table 1. After the polymerization, the crude polymers were reprecipitated in acetone to remove remaining unreacted **PS-Br**. All the polymers showed M_n around 5,000 and broaden PDI. Although the molecular weights of diblock copolymers are relatively low compared to that of PTPA homopolymer, which reaches up to 14,000, the gel

permeation chromatography (GPC) profiles of **PTPA-*b*-PS**s were monomodal with a slight shift toward high molecular weight from that of **PS-Br** (Figure 1). Therefore, we assumed that the formation of **PTPA-*b*-PS** succeeded without contamination of PS homopolymer. The obtained diblock copolymers showed good solubility in common solvents such as chloroform and tetrahydrofuran.

Scheme 2. Synthesis of **PTPA-*b*-PS** via C–N coupling polymerization using **PS-Br** as a terminal modifier.

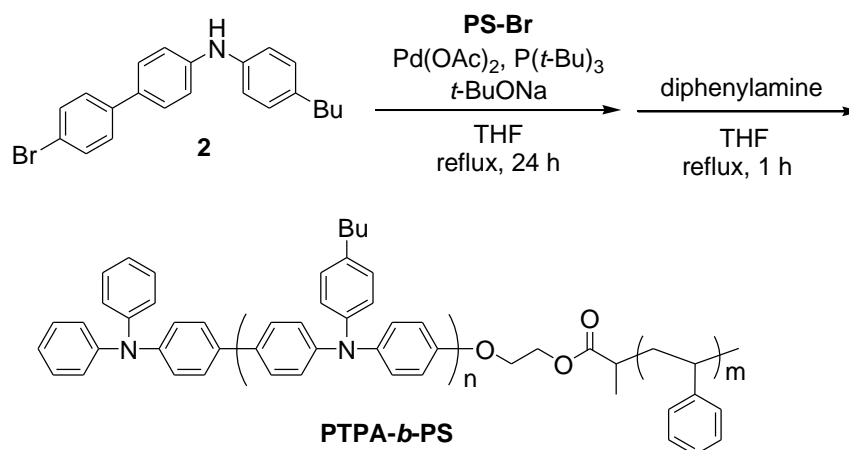
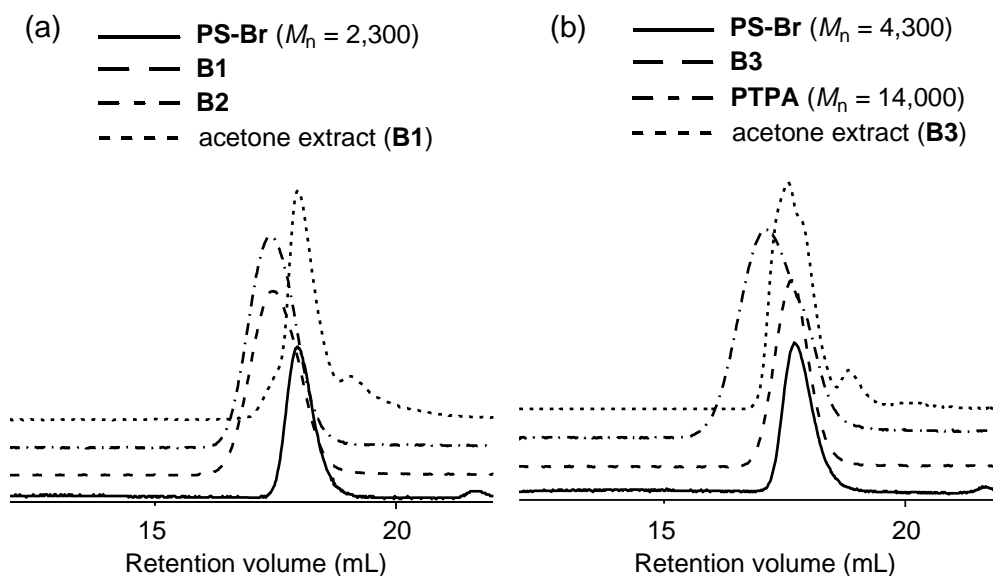


Table 1. Characteristics of **PTPA-*b*-PS** prepared by C–N coupling polymerization.

Polymer	PS-Br M_n (PDI)	M_n^a	M_w^a	PDI ^a	wt. ratio ^b PS:PTPA
B1	2,300 (1.19) ^c	5,000	9,300	1.84	5.3:94.7
B2	2,300 (1.19) ^d	5,000	10,000	1.93	13:87
B3	4,300 (1.18) ^d	4,700	10,000	2.17	39:61

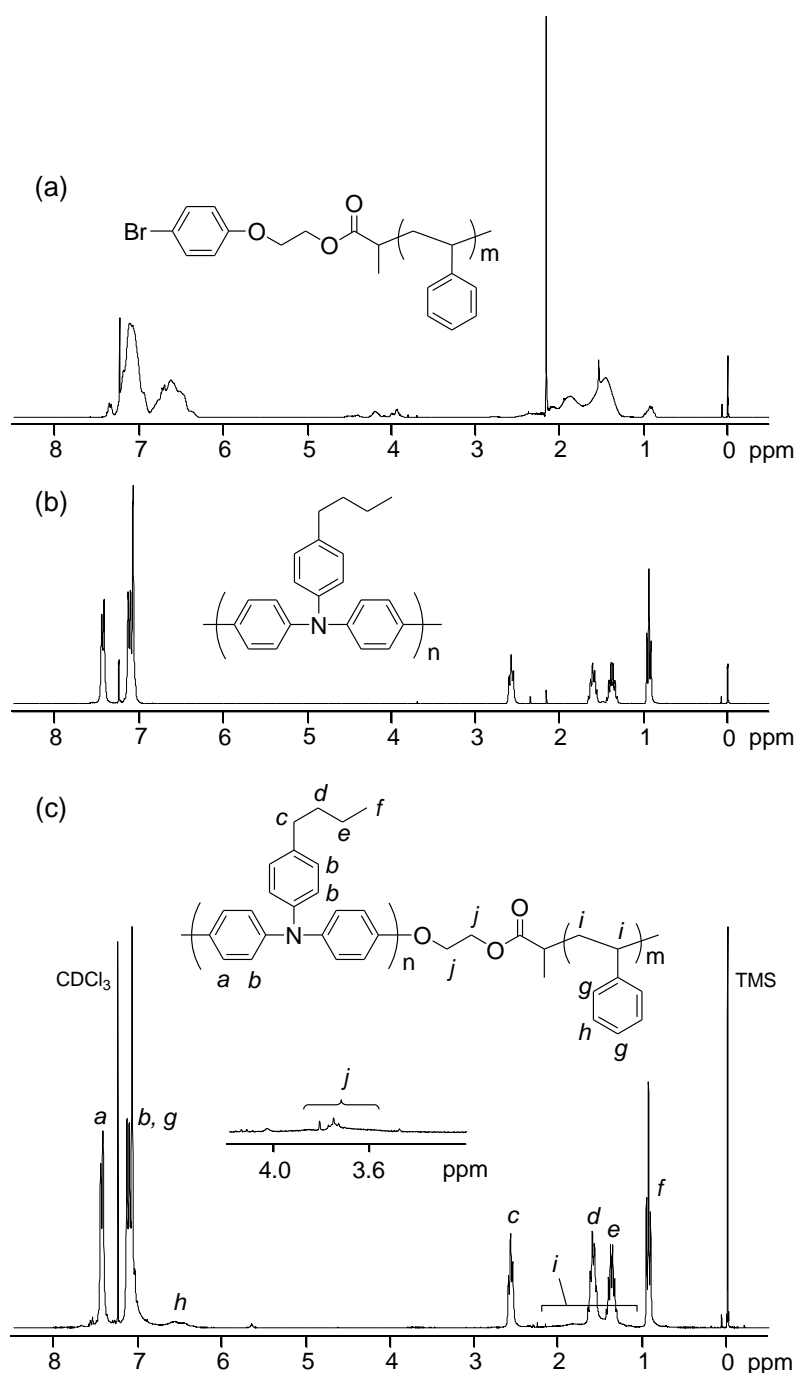
^a Determined by GPC eluted by chloroform with polystyrene standards. ^b Determined by ¹H NMR spectra. ^c 2 mol% to **2** was used for polymerization. ^d 5 mol% to **2** was used for polymerization.

Figure 1. GPC chromatograms of (a) B1 and B2, and (b) B3 compared with PS and PTPA (as control) homopolymers, and the extract in the acetone solution.



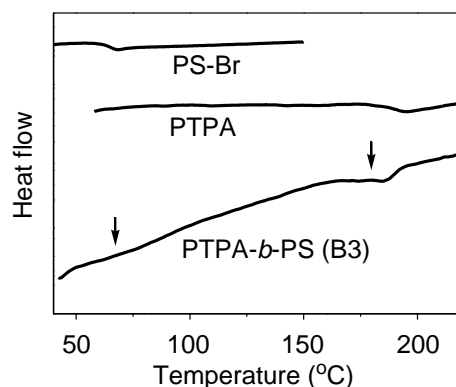
The structures of the diblock copolymers were characterized by ^1H NMR spectra. Figure 2 shows the representative ^1H NMR spectrum of B2 with those of homopolymers. In addition to the signals assignable to PTPA backbone, new signals derived from PS segment appeared at aromatic and aliphatic regions. Furthermore, the signals assignable to methylene units at the junction point were observed at around 3.6 ppm (Figure 2(c), inset), which shifted from those of **PS-Br** at around 4.0 ppm (Figure 2(a)). These results clearly indicate that the PS block was successfully introduced at a terminal of PTPA. The weight ratio of PS was calculated by comparing the integral ratio of *meta* protons of styrene ring (assigned as *h*) at 6.6 ppm with methylene protons of butyl group at 2.6 ppm (assigned as *c*). The weight ratios of PS segment were determined as listed in Table 1, which ranged from 5.3 to 39%.

Figure 2. ^1H NMR spectra of (a) **PS-Br**, (b) PTPA, and (c) **PTPA-*b*-PS (B2)**.



The thermal properties of **PTPA-*b*-PS** were measured by DSC. Figure 3 shows the DSC curve of B3 in the second heating scan. The glass transition temperatures (T_g) were observed at 70 and 180 °C corresponding to those of PS and PTPA homopolymers, respectively. Only one T_g derived from PTPA segment was observed for **PTPA-*b*-PS** with low PS content, B1 and B2.

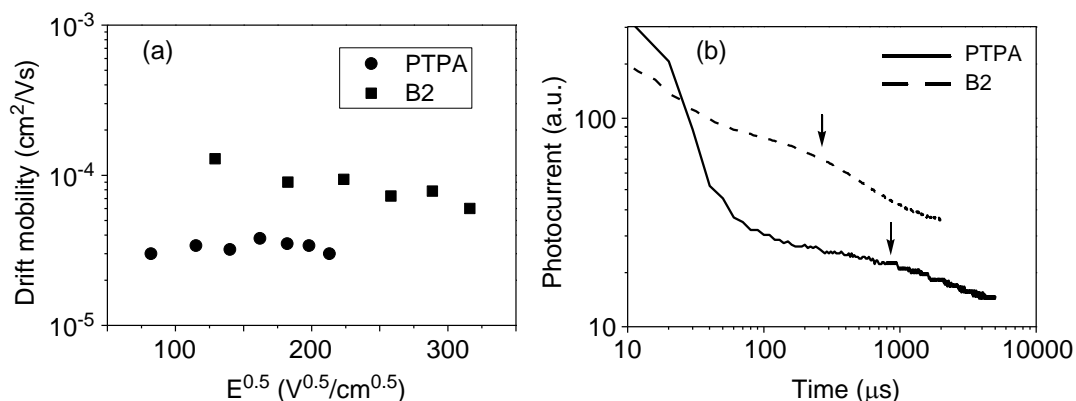
Figure 3. DSC profiles of PS-Br ($M_n = 2,300$), PTPA, and **PTPA-*b*-PS** (B3) in the second heating scan. Arrows indicate the glass transition points of PS and PTPA segments.



2.2. Hole Mobility of Block Copolymer Films

The hole mobility was measured for the block copolymer films by means of time of flight (TOF) method. As a charge generation layer, Ti-phthalocyanine was used. The drift mobilities of PTPA and **PTPA-*b*-PS** (B2) at various electric fields are shown in Figure 4. The hole mobility was almost constant and independent of the electric field for the homopolymer, whereas slightly negative slope was obtained for the block copolymer. This negative electric field dependence of the hole mobility was also observed for an amorphous triphenylamine compound [43]. The block copolymer film showed higher hole mobility than the homopolymer film, which increased up to $1.3 \times 10^{-4} \text{ cm}^2/\text{Vs}$. This finding indicates that the introduction of PS segment does not disturb the charge transportation in the PTPA domain, furthermore, and that a slight increase of the hole mobility was achieved by the presence of PS segment. The inert second block is assumed to attribute to the formation of the defect-free film. Unfortunately, the hole mobility of the block copolymer film with higher PS content (B3) could not be measured because of cracking all over the film.

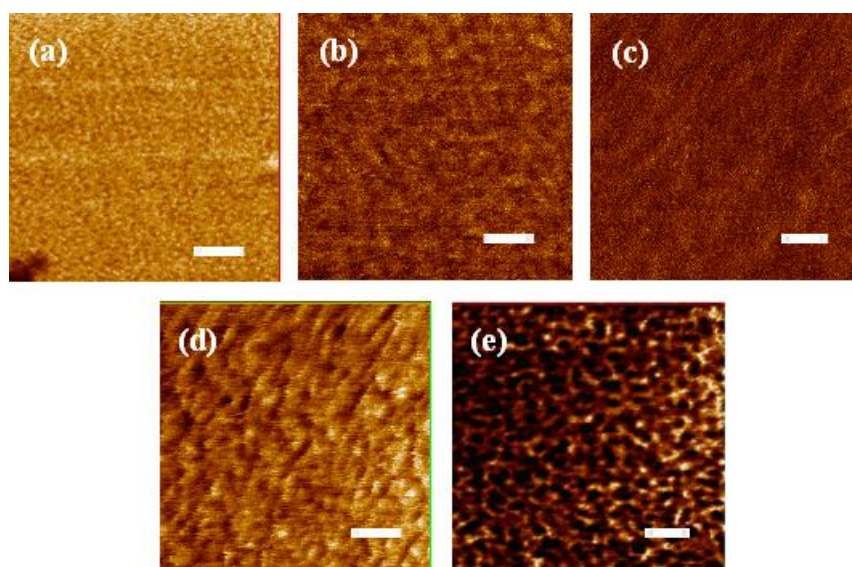
Figure 4. (a) Hole drift mobility at various electric fields and (b) photocurrent transient signals at 40 V.



2.3. Surface Morphology of Blend Films

The thin polymer films blended with fullerene derivative PCBM, a well known electron transporting material, were fabricated on the glass substrate, and the surface morphology of the films was studied by AFM measurement after annealed at 170 °C for 1 h. The weight ratio of polymer:PCBM was fixed as 1:1 for all the blend films. Diblock copolymer **PTPA-*b*-PS** (B3) itself exhibits microphase-separated structure, as shown in Figure 5(a), with the domain size of 10 nm. As a control, PTPA with M_n of 13,000 was blended with PCBM, and the surface morphology of the homopolymer blend film was examined (Figure 5(b)). Slight contrast can be observed at the surface of homopolymer blend film, however, where no clear phase separation occurred. For the diblock copolymer blends, three types of **PTPA-*b*-PS** (B1 to B3) were used to investigate the effect of PS content on the surface morphology of the blend films. When the weight fraction of PS was low (5.3 wt%), the surface became completely homogeneous as shown in Figure 5(c). Increasing the PS content, the surface morphology gradually changed to give a phase-separated structure with the domain size of around 20 nm at 39 wt% of PS content (Figure 5(d,e)). Because the PTPA segment has good compatibility with PCBM, blends films using PTPA homopolymer or B1 showed the homogeneous surface. On the other hand, PS is more compatible component with PCBM than PTPA, which separated PTPA (rich) domain and PS with PCBM (rich) domain at higher PS contents. The black area in the AFM phase image indicates soft domain, therefore, assignable to PS (rich) domain.

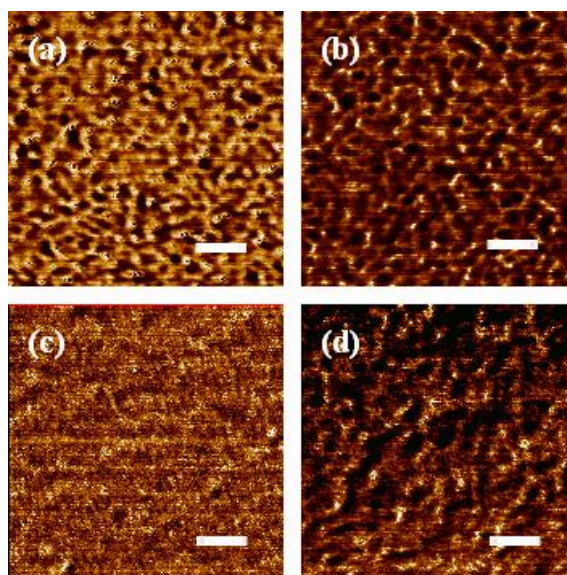
Figure 5. The AFM phase images of the polymer films using (a) B3 only, (b) PTPA with PCBM, (c) B1 with PCBM, (d) B2 with PCBM, and (e) B3 with PCBM. For the blends with PCBM, all the compositions of polymer:PCBM were 1:1 in weight ratio. Bar indicates 100 nm.



In order to investigate the availability of **PTPA-*b*-PS** as a promoter, three-component blend films consisting of **PTPA-*b*-PS** (B3), PTPA, and PCBM were prepared. The compositions of the blends were 15:35:50 and 5:45:50 in the weight ratio, whereas the overall PS contents were 12 and 4 wt%, respectively. The surface of the blend films was observed by AFM before and after annealing

at 170 °C for 1 h (Figure 6). When the weight fraction of B3 was 15 wt% (Figure 6(a,b)), the microphase-separated structure similar to B3/PCBM blend was observed in spite of low overall PS content. The microphase separation already exists at the surface of as-made film, and the average domain size of 20 nm was maintained after annealing process. On the other hand, no microphase separation formed in as-made film using 5 wt% of B3 (Figure 6(c)). After annealing, the phase separation was observed, but the structure was slightly distorted (Figure 6(d)).

Figure 6. The AFM phase images of the blend films consisting of B3:PTPA:PCBM with the weight ratio of 15:35:50 (a) before and (b) after annealing, and with the weight ratio of 5:45:50 (c) before and (d) after annealing. Annealing: 170 °C for 1 h. Bar indicates 100 nm.



2.4. Evaluation of Photovoltaic Device

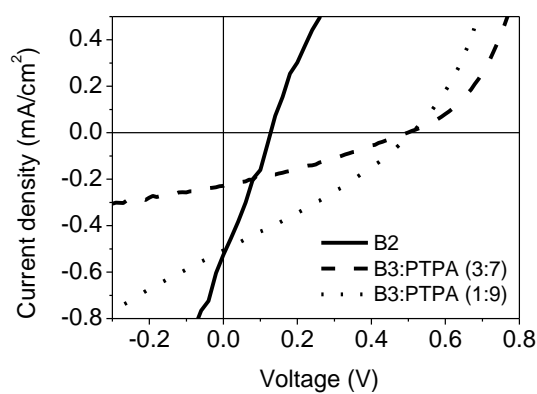
The photovoltaic devices based on the polymer blend systems, PTPA and/or **PTPA-*b*-PS** blended with PCBM in 1:1 weight ratio, were fabricated to evaluate the I-V characteristics as shown in Figure 7. The devices were constructed as the following structure: ITO/PEDOT:PSS (30 nm)/polymer blend (70 nm)/LiF (0.5 nm)/Al (100 nm). The results using the various polymers are summarized in Table 2. Homopolymer (PTPA) blend film showed no photovoltaic characteristic. When the **PTPA-*b*-PSs** with different PS contents were used, only the device based on B2 (PS content: 13 wt%) exhibited photovoltaic characteristics. However, the open circuit voltage (V_{oc}) and the fill factor were low. Because the blend film of B1 as well as PTPA showed homogeneous morphology in AFM observation, where the charge recombination may frequently occur in the donor-acceptor mixture within a molecular size, a photocurrent was not obtained from these devices. On the other hand, the device based on B3 also showed no photocurrent due to the high PS contents, which caused the insulation for charge transportation. The three-component blend consisting of PTPA, **PTPA-*b*-PS** (B3), and PCBM were utilized for the active layer of the device. The device performances were improved by using three-component blends compared with block copolymer blend using B2. By adding B3 to the blend of PTPA and PCBM, the morphology in the active layer changed to the microphase-separated structure, as revealed in AFM images, without the content of PS increased. Because PTPA backbone

can absorb the light only below 400 nm, the efficiency was quite low for all the devices. Chemical modification of PTPA backbone for the improvement of absorption range is under investigation.

Table 2. The performance of the photovoltaic devices based on PTPA polymers.

Polymer	V_{oc} (V)	J_{sc} (mA/cm ²)	Efficiency (%)	Fill Factor (%)
B2	0.14	0.53	0.013	18.0
B3+PTPA(3:7)	0.50	0.28	0.034	29.9
B3+PTPA(1:9)	0.52	0.50	0.077	29.2

Figure 7. I-V characteristics of the devices based on PTPA polymers blended with PCBM in 1:1 weight ratio.



3. Experimental Section

3.1. Materials

Tetrahydrofuran (THF) was used as distilled over sodium and benzophenone. Toluene was distilled over calcium hydride and stored under nitrogen. Styrene was used as freshly distilled over calcium hydride under reduced pressure. 2-(4-Bromophenoxy)ethanol was prepared from 4-bromophenol and 2-chloroethanol according to the reference [44]. 4-(4'-Bromophenyl)-4''-butyldiphenylamine (**2**) was prepared from 4,4'-dibromobiphenyl and 4-butyraniline according to the previous report [40]. The other reagents were used as received.

3.2. Synthesis of 2-(4-Bromophenoxy)ethyl 2-Bromopropionate (**1**)

To a flask equipped with a stopcock were added 2-(4-bromophenoxy)ethanol (0.438 g, 2.01 mmol), pyridine (1.20 mL), and THF (15.0 mL) at 0 °C under nitrogen. After 2-bromopropionyl bromide (0.492 g, 2.30 mmol) was added dropwise, the mixture was stirred for 30 min at 0 °C and for 24 h at room temperature. THF was removed by rotary evaporator, and the residue was extracted by chloroform and water. The organic layer was dried with magnesium sulfate and concentrated by rotary evaporator. The crude product was purified by column chromatography eluted with hexane:ethyl acetate = 1:1 to give yellow liquid. The yield was 0.480 g (68.2%).

3.3. Synthesis of Polystyrene Using **1** as an Initiator (**PS-Br**)

To a Schlenk tube were added **1** (0.10 g, 0.285 mmol), styrene (3.30 mL, 28.5 mmol), copper (I) bromide (41.7 mg, 0.290 mmol), copper (II) bromide (6.4 mg, 0.0285 mmol), and *N,N,N',N',N''*-pentamethyldiethylenetriamine (PMDETA, 0.0593 mL, 0.284 mmol), and anisole (2.00 mL) under nitrogen. The mixture was subjected to freeze-thaw cycles to eliminate the air contamination, and stirred for 3 h at 95 °C. After small amount of THF, the solution was poured in methanol. The precipitate was filtered, and purified by the reprecipitation in methanol twice to give white powder. The yield was 1.66 g (54.1%).

3.4. Preparation of Poly(4-butyltriphenylamine)-*b*-Polystyrene (**PTPA-b-PS**)

To a two-necked flask equipped with a stopcock and a condenser were added **2** (0.60 g, 1.57 mmol), sodium *t*-butoxide (0.152 g, 1.58 mmol), and THF (3.00 mL) under nitrogen. The solution of PS-Br (0.367 g, 0.0857 mmol), palladium (II) acetate (7.1 mg, 0.0176 mmol), and tri-*t*-butylphosphine (30.0 mL) in THF (2.00 mL) was prepared in another flask equipped with a stopcock under nitrogen, stirred for 30 min at room temperature, and added to the solution of **2** by a syringe in one portion. The mixture was stirred for 24 h at reflux temperature. The solution of diphenylamine (0.0267 g, 0.157 mmol) in THF (0.6 mL) was added to the solution, and additional stirring for 1 h was performed. The resulting solution was poured into methanol, and the precipitate was filtered. The polymer was reprecipitated in acetone. After the filtration and drying, pale greenish polymer was obtained. The yield was 0.568 g, 41.6%).

3.5. Measurement of Hole Mobility (Time of Flight Method)

Aluminum (150 nm) was vacuum-deposited on a well-cleaned glass slide as an anode. Thin charge generating layer was laminated on aluminum by spin-coating from chloroform solution of titanium phthalocyanine at a rate of 2,500 rpm for 30 s. Sequentially, the polymer layer was deposited by bar-coating from 20 wt% of 1,1,2,2-tetrachloroethane solution. The thickness of the polymer layer was in a range of 9 to 10 μm. After the polymer layer was dried in vacuum, the semi-transparent gold layer was sputtered on the polymer layer as a cathode. The pulsed light was illuminated on the device to generate charges in the phthalocyanine layer by a xenon lamp, and the photocurrent was recorded on an oscilloscope.

3.6. Photovoltaic Device Evaluation

Prior to preparation of devices, a glass slide with indium tin oxide (ITO) patterns was washed by an alkaline cleaner under sonication and rinsed with deionized water. The substrate was subsequently washed by 2-propanol under sonication, rinsed with clean 2-propanol, and dried with nitrogen. PEDOT:PSS with 30 nm of thickness was spin-coated on the substrate at 2500 rpm for 30 s from the dispersion in water filtered by 0.2 μm of membrane filter, followed by annealing at 200 °C for 1 h. Polymer blend layer was laminated on PEDOT:PSS by spin-coating at 1,000 rpm for 30 s from 1,1,2-trichloroethane solution (10 mg/mL) filtered by 0.2 μm of membrane filter, and annealed at 170 °C for 1 h under nitrogen atmosphere. As a cathode, lithium fluoride with 0.5 nm of thickness

followed by aluminum with 100 nm of thickness was vacuum-deposited on the polymer layer at a rate of 0.1 Å/s and a rate of 4.5 Å/s using tantalum and tungsten boats, respectively. A typical size of the photo-active area was 4 mm². The photocurrent-voltage characteristic was measured upon the exposure of the light by a xenon lamp with 100 mW/cm².

3.7. Measurements

¹H and ¹³C NMR spectra were obtained on a JEOL ALPHA500 instrument at 500 and 125 MHz, respectively. Deuterated chloroform was used as a solvent with tetramethylsilane as an internal standard. Number- and weight-average molecular weights (M_n and M_w) were determined by gel permeation chromatography (GPC) analysis with a JASCO RI-2031 detector eluted with chloroform at a flow rate of 1.0 mL min⁻¹ and calibrated by standard polystyrene samples. Differential scanning calorimetry (DSC) analyses were performed on a Rigaku DSC-8230 under a nitrogen atmosphere at heating and cooling rates of 10 °C/min. Atomic force microscopy (AFM) measurements were performed on a JEOL JSPM-4200 system in tapping mode (phase and topographic modes) with an MPP-11100-10 silicon probe (resonant frequency: 300 kHz, force constant: 40 N/m). All thin films of polymers were spin-cast onto glass slide by a MIKASA 1H-D7 spin coater from 1,1,2,2-tetrachloroethane solutions at 1,500 rpm for 30 s.

4. Conclusions

The novel block copolymers based on the triphenylamine backbone, PTPA-*b*-PS, with various contents of PS were prepared via ATRP of styrene, followed by C-N coupling polymerization. Chemical structures and the compositions of block copolymers were confirmed by ¹H NMR spectra. The T_g s derived from PTPA and PS segments were observed in DCS analysis of PTPA-*b*-PS, indicating the phase separation of block copolymers. The hole mobility of the PTPA-*b*-PS film was found to be higher than that of PTPA film by TOF method. The surface morphologies of the blend film composed of the block copolymer and PCBM were investigated by AFM measurement. The blend films using block copolymer with higher molecular weight polystyrene showed the microphase-separated structure with a domain size of around 20 nm. Finally, the photovoltaic devices consisting of PTPA, PTPA-*b*-PS, and PCBM showed higher efficiency than the device based on homopolymer blend, which provides a reasonable correlation with the morphological change in AFM measurement. These results indicate that the control of morphology in thin film devices can be achieved by using block copolymer consisting of charge transporting segments.

References

1. Blom, P.W.M.; Mihailetschi, V.D.; Koster, L.J.A.; Markov, D.E. Device physics of polymer: Fullerene bulk heterojunction solar cells. *Adv. Mater.* **2007**, *19*, 1551-1566.
2. Thompson, B.C.; Frechet, J.M.J. Organic photovoltaics—Polymer-fullerene composite solar cells. *Angew. Chem. Int. Ed.* **2008**, *47*, 58-77.

3. Li, G.; Shrotriya, V.; Huang, J. S.; Yao, Y.; Moriarty, T.; Emery, K.; Yang, Y. High-efficiency solution processable polymer photovoltaic cells by self-organization of polymer blends. *Nat. Mater.* **2005**, *4*, 864-868.
4. Ma, W.L.; Yang, C.Y.; Gong, X.; Lee, K.; Heeger, A.J. Thermally stable, efficient polymer solar cells with nanoscale control of the interpenetrating network morphology. *Adv. Funct. Mater.* **2005**, *15*, 1617-1622.
5. Shrotriya, V.; Yao, Y.; Li, G.; Yang, Y. Effect of self-organization in polymer/fullerene bulk heterojunctions on solar cell performance. *Appl. Phys. Lett.* **2006**, *89*, 063505.
6. Campoy-Quiles, M.; Ferenczi, T.; Agostinelli, T.; Etchegoin, P.G.; Kim, Y.; Anthopoulos, T.D.; Stavrinou, P.N.; Bradley, D.D.C.; Nelson, J. Morphology evolution via self-organization and lateral and vertical diffusion in polymer: Fullerene solar cell blends. *Nat. Mater.* **2008**, *7*, 158-164.
7. Huang, W.Y.; Huang, P.T.; Han, Y.K.; Lee, C.C.; Hsieh, T.L.; Chang, M.Y. Aggregation and gelation effects on the performance of poly(3-hexylthiophene)/fullerene solar cells. *Macromolecules* **2008**, *41*, 7485-7489.
8. Li, G.; Shrotriya, V.; Yao, Y.; Huang, J.S.; Yang, Y. Manipulating regioregular poly(3-hexylthiophene): [6,6]-phenyl-C₆₁-butyric acid methyl ester blends—route towards high efficiency polymer solar cells. *J. Mater. Chem.* **2007**, *17*, 3126-3140.
9. Kim, Y.; Choulis, S.A.; Nelson, J.; Bradley, D.D.C.; Cook, S.; Durrant, J.R. Device annealing effect in organic solar cells with blends of regioregular poly(3-hexylthiophene) and soluble fullerene. *Appl. Phys. Lett.* **2005**, *86*, 063502.
10. Li, G.; Shrotriya, V.; Yao, Y.; Yang, Y. Investigation of annealing effects and film thickness dependence of polymer solar cells based on poly(3-hexylthiophene). *J. Appl. Phys.* **2005**, *98*, 043704.
11. Reyes-Reyes, M.; Kim, K.; Carroll, D.L. High-efficiency photovoltaic devices based on annealed poly(3-hexylthiophene) and 1-(3-methoxycarbonyl)-propyl-1-phenyl-(6,6)C₆₁ blends. *Appl. Phys. Lett.* **2005**, *87*, 083506.
12. Ko, C.J.; Lin, Y.K.; Chen, F.C. Microwave annealing of polymer photovoltaic devices. *Adv. Mater.* **2007**, *19*, 3520-3523.
13. Li, G.; Yao, Y.; Yang, H.; Shrotriya, V.; Yang, G.; Yang, Y. “Solvent annealing” effect in polymer solar cells based on poly(3-hexylthiophene) and methanofullerenes. *Adv. Funct. Mater.* **2007**, *17*, 1636-1644.
14. Sommer, M.; Huettner, S.; Thelakkat, M. Donor-acceptor block copolymers for photovoltaic applications. *J. Mater. Chem.* **2010**, *20*, 10788-10797.
15. Lindner, S.M.; Hüttner, S.; Chiche, A.; Thelakkat, M.; Krausch, G. Charge separation at self-assembled nanostructured bulk interface in block copolymers. *Angew. Chem. Int. Ed.* **2006**, *45*, 3364-3368.
16. Sivula, K.; Ball, Z.T.; Watanabe, N.; Frechet, J.M.J. Amphiphilic diblock copolymer compatibilizers and their effect on the morphology and performance of polythiophene: Fullerene solar cells. *Adv. Mater.* **2006**, *18*, 206-210.

17. Barrau, S.; Heiser, T.; Richard, F.; Brochon, C.; Ngov, C.; van de Wetering, K.; Hadziioannou, G.; Anokhin, D.V.; Ivanov, D.A. Self-assembling of novel fullerene-grafted donor-acceptor rod-coil block copolymers. *Macromolecules* **2008**, *41*, 2701-2710.
18. Sommer, M.; Lang, A.S.; Thelakkat, M. Crystalline-crystalline donor-acceptor block copolymers. *Angew. Chem. Int. Ed.* **2008**, *47*, 7901-7904.
19. Zhang, Y.; Tajima, K.; Hirota, K.; Hashimoto, K. Synthesis of all-conjugated diblock copolymers by quasi-living polymerization and observation of their microphase separation. *J. Am. Chem. Soc.* **2008**, *130*, 7812-7813.
20. Brochon, C.; Sary, N.; Mezzenga, R.; Ngov, C.; Richard, F.; May, M.; Hadziioannou, G. Synthesis of poly(paraphenylene vinylene)-polystyrene-based rod-coil block copolymer by atom transfer radical polymerization: Toward a self-organized lamellar semiconducting material. *J. Appl. Polym. Sci.* **2008**, *110*, 3664-3670.
21. Tam, W.Y.; Mak, C.S.K.; Ng, A.M.C.; Djuricic, A.B.; Chan, W.K. Multifunctional poly(*n*-vinylcarbazole)-based block copolymers and their nanofabrication and photosensitizing properties. *Macromol. Rapid Commun.* **2009**, *30*, 622-626.
22. Botiz, I.; Darling, S.B. Self-assembly of poly(3-hexylthiophene)-*block*-polylactide block copolymer and subsequent incorporation of electron acceptor material. *Macromolecules* **2009**, *42*, 8211-8217.
23. Chueh, C.C.; Higashihara, T.; Tsai, J.H.; Ueda, M.; Chen, W. C. All-conjugated diblock copolymer of poly(3-hexylthiophene)-*block*-poly(3-phenoxyethylthiophene) for field-effect transistor and photovoltaic applications. *Org. Electron.* **2009**, *10*, 1541-1548.
24. Sommer, M.; Huttner, S.; Steiner, U.; Thelakkat, M. Influence of molecular weight on the solar cell performance of double-crystalline donor-acceptor block copolymers. *Appl. Phys. Lett.* **2009**, *95*, 183308.
25. Zhang, Q.L.; Cirpan, A.; Russell, T.P.; Emrick, T. Donor-acceptor poly(thiophene-*block*-perylene diimide) copolymers: Synthesis and solar cell fabrication. *Macromolecules* **2009**, *42*, 1079-1082.
26. Rajaram, S.; Armstrong, P.B.; Kim, B.J.; Frechet, J.M.J. Effect of addition of a diblock copolymer on blend morphology and performance of poly(3-hexylthiophene):perylene diimide solar cells. *Chem. Mater.* **2009**, *21*, 1775-1777.
27. Dante, M.; Yang, C.; Walker, B.; Wudl, F.; Nguyen, T.Q. Self-assembly and charge-transport properties of a polythiophene-fullerene triblock copolymer. *Adv. Mater.* **2010**, *22*, 1835-1839.
28. Tsai, J.H.; Lai, Y.C.; Higashihara, T.; Lin, C.J.; Ueda, M.; Chen, W.C. Enhancement of P3HT/PCBM photovoltaic efficiency using the surfactant of triblock copolymer containing poly(3-hexylthiophene) and poly(4-vinyltriphenylamine) segments. *Macromolecules* **2010**, *43*, 6085-6091.
29. Sary, N.; Richard, F.; Brochon, C.; Leclerc, N.; Leveque, P.; Audinot, J.N.; Berson, S.; Heiser, T.; Hadziioannou, G.; Mezzenga, R. A new supramolecular route for using rod-coil block copolymers in photovoltaic applications. *Adv. Mater.* **2010**, *22*, 763-768.
30. Yu, W.L.; Pei, J.; Huang, W.; Heeger, A.J. A novel triarylamine-based conjugated polymer and its unusual light-emitting properties. *Chem. Commun.* **2000**, doi: 10.1039/A909857G.
31. Michinobu, T.; Osako, H.; Shigehara, K. Alkyne-linked poly(1,8-carbazole)s: A novel class of conjugated carbazole polymers. *Macromol. Rapid Commun.* **2008**, *29*, 111-116.

32. Sek, D.; Iwan, A.; Jarzabek, B.; Kaczmarczyk, B.; Kasperczyk, J.; Mazurak, Z.; Domanski, M.; Karon, K.; Lapkowski, M. Hole transport triphenylamine-azomethine conjugated system: Synthesis and optical, photoluminescence, and electrochemical properties. *Macromolecules* **2008**, *41*, 6653-6663.
33. Natori, I.; Natori, S.; Usui, H.; Sato, H. Anionic polymerization of 4-diphenylaminostyrene: Characteristics of the alkyllithium/*N,N,N',N'*-tetramethylethylenediamine system for living anionic polymerization. *Macromolecules* **2008**, *41*, 3852-3858.
34. Lin, K.R.; Chien, Y.H.C.; Chang, C.C.; Hsieh, K.H.; Leung, M.K. Synthesis, electrochemical behavior, and electronic properties of hyperbranched poly(*p*-methylenetriphenylamine): An unexpected condensation polymerization from *N*-[4-(Tosyloxybutyloxymethyl)phenyl]-*N,N*-diphenylamine. *Macromolecules* **2008**, *41*, 4158-4164.
35. Dumsch, I.; Kudla, C.J.; Scherf, U. Polytriarylamines with on-chain crystal violet moieties. *Macromol. Rapid Commun.* **2009**, *30*, 840-844.
36. Michinobu, T.; Kumazawa, H.; Otsuki, E.; Usui, H.; Shigehara, K., Synthesis and properties of nitrogen-linked poly(2,7-carbazole)s as hole-transport material for organic light emitting diodes. *J. Polym. Sci. A Polym. Chem.* **2009**, *47*, 3880-3891.
37. Tsuchiya, K.; Sakaguchi, K.; Kasuga, H.; Kawakami, A.; Taka, H.; Kita, H.; Ogino, K. Synthesis of charge transporting block copolymers containing 2,7-dimethoxycarbazole units for light emitting device. *Polymer* **2010**, *51*, 616-622.
38. Ogino, K.; Kanegae, A.; Yamaguchi, R.; Sato, H.; Kurjata, J. Oxidative coupling polymerization of 4-methyltriphenylamine. *Macromol. Rapid Commun.* **1999**, *20*, 103-106.
39. Takahashi, C.; Moriya, S.; Fugono, N.; Lee, H.C.; Sato, H. Preparation and characterization of poly(4-alkyltriphenylamine) by chemical oxidative polymerization. *Synth. Met.* **2002**, *129*, 123-128.
40. Tsuchiya, K.; Shimomura, T.; Ogino, K. Preparation of diblock copolymer based on poly(4-*n*-butyltriphenylamine) via palladium coupling polymerization. *Polymer* **2009**, *50*, 95-101.
41. Gu, Z.; Kanto, T.; Tsuchiya, K.; Ogino, K. Synthesis of poly(3-hexylthiophene)-*b*-poly(ethylene oxide) for application to photovoltaic device. *J. Photopolym. Sci. Technol.* **2010**, *23*, 405-406.
42. Maeda, Y.; Shimoi, Y.; Ogino, K. Fabrication of microporous films utilizing amphiphilic block copolymers and their use as templates in poly(aniline) preparation. *Polym. Bull.* **2005**, *53*, 315-321.
43. Kageyama, H.; Ohnishi, K.; Nomura, S.; Shirota, Y. Negative electric-field dependence of hole drift mobility for a molecular glass of tri(*o*-terphenyl-4-yl)amine. *Chem. Phys. Lett.* **1997**, *277*, 137-141.
44. Inokuma, S.; Kimura, K.; Funaki, T.; Nishimura, J. Synthesis of pyridinocrownphanes exhibiting high Ag⁺-affinity. *Heterocycles* **2001**, *54*, 123-130.